THE JOURNAL OF BIOLOGICAL CHEMISTRY VOL. 286, NO. 17, pp. 15332–15343, April 29, 2011

Role of YKL-40 in the Angiogenesis, Radioresistance, and Progression of Glioblastoma*[S]

Received for publication, December 14, 2010, and in revised form, February 28, 2011 Published, JBC Papers in Press, March 8, 2011, DOI 10.1074/jbc.M110.212514

Ralph A. Francescone[‡], Steve Scully[‡§], Michael Faibish[‡], Sherry L. Taylor[¶], Dennis Oh[¶], Luis Moral[‖], Wei Yan[‡], Brooke Bentley[§], and Rong Shao[‡§1]**

*From the [‡]Molecular and Cellular Biology Program, Morrill Science Center, and the **Department of Veterinary and Animal Sciences, University of Massachusetts, Amherst, Massachusetts 01003, the [§]Pioneer Valley Life Sciences Institute, University of Massachusetts Amherst, Springfield, Massachusetts 01107, and the Departments of [¶]Neurosurgery and [‖]Pathology, Baystate Medical Center, Tufts University, Springfield, Massachusetts 01199*

Glioblastoma is one of the most fatal cancers, characterized by a strong vascularized phenotype. YKL-40, a secreted glycoprotein, is overexpressed in patients with glioblastomas and has potential as a novel tumor biomarker. The molecular mechanisms of YKL-40 in glioblastoma development, however, are poorly understood. Here, we aimed to elucidate the role YKL-40 plays in the regulation of VEGF expression, tumor angiogenesis, and radioresistance. YKL-40 up-regulated VEGF expression in glioblastoma cell line U87, and both YKL-40 and VEGF synergistically promote endothelial cell angiogenesis. Interestingly, long term inhibition of VEGF up-regulated YKL-40. YKL-40 induced coordination of membrane receptor syndecan-1 and integrin $\alpha v\beta 5$, and triggered a signaling cascade through FAK^{397} to ERK-1 and ERK-2, leading to elevated VEGF and enhanced angiogenesis. In addition, γ-irradiation of U87 cells increased YKL-40 expression that protects cell death through AKT activation and also enhances endothelial cell angiogenesis. Blockade of YKL-40 activity or expression decreased tumor growth, angiogenesis, and metastasis in xenografted animals. Immunohistochemical analysis of human glioblastomas revealed a correlation between YKL-40, VEGF, and patient survival. These findings have shed light on the mechanisms by which YKL-40 promotes tumor angiogenesis and malignancy, and thus provide a therapeutic target for tumor treatment.

Tumor angiogenesis, a process of new vasculature formation, is of paramount importance in solid tumor development (1). The supply of new blood vessels in tumors not only supports autonomous tumor proliferation but also aids in removing accumulated waste from extensive metabolism that would normally induce necrosis. A number of angiogenic factors such as VEGF, bFGF, and a recently identified secreted glycoprotein YKL-40 (also known as human cartilage glycoprotein-39) have been known to play critical roles in the development of the tumor vasculature (2–4). Thus, they presumably function through synergistic action to give rise to a robust angiogenic phenotype.

YKL-40, a member of the chitinase-like glycoprotein family, was first identified from the medium of human osteosarcoma cell line MG-63 (5). Structural analysis has demonstrated that YKL-40 contains highly conserved chitin-binding domains; however, it functionally lacks the ability to act as a chitinase because of a mutation of an essential glutamic acid residue to leucine in the chitinase-3-like catalytic domain (6, 7). Although the physiological role of YKL-40 is not completely understood, it is conceivable that YKL-40 is linked with proliferation of connective tissues and activation of vascular endothelial cells (8–10). Growing clinical evidence has indicated that aberrant expression of YKL-40 is largely associated with the pathogenesis of a variety of human diseases. For example, YKL-40 levels are elevated in the blood serum of patients with chronic inflammatory diseases such as rheumatoid- and osteoarthritis, hepatic fibrosis, and asthma (11–15), which is suggestive of its pathological function associated with extracellular matrix remodeling. Over the past decade, mounting clinical studies have demonstrated a correlation of elevated serum levels of YKL-40 with aggressive cancers and poorer survival in carcinomas of the breast, colon, ovary, and brain (16–22), suggesting that serum levels of YKL-40 serve as a diagnostic and prognostic biomarker. Recently, we found that YKL-40 is capable of stimulating angiogenesis of microvascular endothelial cells in breast cancer (2). In addition, YKL-40-induced angiogenesis is dependent on the interaction between membrane receptors syndecan-1 (Syn-1)[2] and integrin $\alpha v\beta 3$. These findings have shed light onto the mechanisms through which YKL-40 prompts breast cancer development.

Vascular endothelial growth factor (VEGF) is believed to be a primary promoter of angiogenesis (23). VEGF binds to two tyrosine kinase membrane receptors, VEGFR-1 (known as Flt-1) and VEGFR-2 (also named as Flk-1). Flk-1 acts as a primary receptor mediating VEGF-induced angiogenesis (24–26). Upon binding of VEGF, Flk-1 is activated by autophosphorylation of specific tyrosine residues, followed by binding and activation of Src or proteins containing a Src homology domain 2 (27). Consequently, these mediators activate multiple downstream effectors, including FAK and MAPK (28, 29). Clinic evidence shows that elevated serum levels of VEGF are related to

* This work was supported, in whole or in part, by National Institutes of Health Grant R01 CA120659 from the NCI (to R. S.).

[S] The on-line version of this article (available at http://www.jbc.org) contains supplemental Figs. S1–S3.

[1] To whom correspondence should be addressed: Pioneer Valley Life Sciences Institute, University of Massachusetts Amherst, Springfield, MA 01107. Fax: 413-794-0857; E-mail: rong.shao@bhs.org.

[2] The abbreviations used are: Syn-1, syndecan-1; HMVECs, human microvascular endothelial cells; mAY, monoclonal anti-YKL-40 antibody; IHC, immunohistochemistry; Gy, gray.

decreased survival in patients with breast cancers and brain tumors (30, 31).

Glioblastoma is the most deadly and aggressive type of brain tumor with a median survival time of 12–15 months. It is characterized by highly vascularized tumors and resistance to radio/chemotherapy (32). YKL-40 is one of the most overexpressed proteins in glioblastoma (33–35) and its level correlates with tumor radioresistance and short survival (16). Interestingly, elevated VEGF in glioblastoma is also associated with tumor angiogenesis (36–38). However, clinical trials testing anti-VEGF antibody bevacizumab (Avastin) in recurrent glioblastoma show minimal overall benefit to survival (39, 40). Consistent with these results, there is strong evidence in murine models indicating that anti-VEGF therapy alone resulted in opposite outcomes in which angiogenic and malignant tumors unexpectedly developed (37, 41), suggesting that other angiogenic factors may contribute to this evasive mechanism. This hypothesis was partially supported by the evidence that blockade of *VEGF* via siRNA gene knockdown up-regulates the *YKL-40* transcript (42). However, it remains to be determined for the regulatory relationship between YKL-40 and VEGF, and substantial molecular mechanisms underlying tumor radioresistance and angiogenesis, the hallmark of aggressive glioblastomas. In this study, we found that YKL-40 up-regulated VEGF, and both acted as potent angiogenic factors to exert synergistic effects on angiogenesis in the establishment of tumor malignancy. Moreover, YKL-40 protected tumor cell death induced by γ-irradiation. Elucidation of the molecular mechanisms of YKL-40 may give rise to considerable promise in devising novel therapeutic strategies designed to target YKL-40 in concert with traditional anti-VEGF therapy.

EXPERIMENTAL PROCEDURES

Cell Culture—U87 cells (ATCC, Manassas, VA) and SNB-75 cells (NCI, Frederick, MD) were grown in DMEM supplemented with 10% FBS and penicillin/streptomycin. Human microvascular endothelial cells (HMVEC) were grown in EBM-2 (Lonza, Allendale, NJ) supplemented with 5 μg/ml of hydrocortisone, 5 μg/ml of insulin, 10 ng/ml of hEGF, 10% FBS and penicillin/streptomycin.

RT-PCR—Total RNA from cells was extracted with Tri-Reagent (Molecular Research Inc., Cincinnati, OH). RNA concentration and purity were determined spectrophotometrically ($A_{260/280}$). cDNAs with poly(A) tails were subsequently synthesized through a reverse transcriptional reaction in the presence of oligo$(dT)_{15}$ (Promega, Madison, WI). A fragment of *VEGF* and *GAPDH* DNA was synthesized by a polymerase chain reaction with sense primer, 5′-CTTTCTGCTGTCTTGGGTGC-3′ and antisense primer, 5′-GTGCTGTAGGAAGCTCATCTCTCC-3′; and sense primer, 5′-ATGGGGAAGGTGAAGGTCGGA-3′ and antisense primer, 5′-CTCCTTGGAGGCCATGT-3′, respectively.

Immunoprecipitation and Immunoblotting—Cell lysate samples were processed as described previously (2). Briefly, cell lysates were then incubated with either an anti-integrin β5 or integrin β3 antibody (Chemicon International, Temecula, CA) at 4 °C overnight followed by incubation with protein A-Sepharose beads at 4 °C for 4 h. The immunocomplex was extensively washed and the samples were subjected to running SDS-PAGE. PVDF membranes were incubated with one of a series of primary antibodies against YKL-40, VEGF (Sigma), Syn-1 (Santa Cruz Biotechnology, Santa Cruz, CA), $pFAK^{397}$ (BIOSOURCE, Camarillo, CA), FAK, pERK, ERK (Santa Cruz), pAKT and AKT (Cell Signaling, Beverly, MA), PI3K (Upstate Biotech, Lake Placid, NY), or actin (Sigma). Membranes were then incubated with goat anti-mouse or anti-rabbit secondary antibodies (The Jackson Laboratory, Bar Harbor, ME). Specific signals were detected by enhanced chemiluminescence (VWR, Rockford, IL).

YKL-40 Gene Knockdown—DNA oligos (19 bp) specifically targeting the N-terminal (siRNA 1) or C-terminal (siRNA 2) regions of *YKL-40* were selected and then templates (64 oligo nucleotides) containing these oligos were subcloned into a retroviral pSUPER-puro-vector (OligoEngine, Seattle, WA). 293T retroviral packaging cells were transfected with pSUPER siRNA constructs in the presence of pCL 10A1 vector using FuGENE 6 (Roche Applied Science). Forty-eight hours after transfection, the supernatant was harvested and filtered through 0.45-μm pore size filter and then the viral medium was used to infect U87 cells. Selection with 1 μg/ml of puromycin was started 48 h after infection and puromycin-resistant cell populations were used for subsequent studies.

Tube Formation Assays—HMVECs (1×10^4cells) were transferred onto 96-well Matrigel (BD Bioscience, San Jose, CA) in the presence of conditioned medium of tumor cells with or without neutralizing antibody treatments. After 16 h of incubation, tube-forming structures were analyzed. Images were analyzed with an inverted microscope. Averages of tubules were calculated from three fields in each sample.

Irradiation of Cells and Live/Dead Assay—U87 cell lines were exposed to 0–10 Gy γ-irradiation from a radioactive cesium source. To assay cell viability, the live/dead assay (Invitrogen) was employed. Briefly, 48 or 96 h after γ-irradiation, cells were incubated with the live/dead mixture (calcein AM and ethidium homodimer) to assess the number of live and dead cells. Fluorescent images of live (green) and dead (red) cells were analyzed. The percentages of live and dead cells were quantified.

PI3K Activity—Freshly isolated cell lysates were subjected to measuring kinase activity according to the manufacturer's instructions (Millipore Inc., Bedford, MA).

Tumor Xenografts in Mice—All animal experiments were performed under the approval of the Institutional Animal Care and Use Committee of the University of Massachusetts. SCID/Beige mice were subcutaneously injected with U87 ($5–7.5 \times 10^6$) or SNB-75 (5×10^6) cells in 0.2 ml of PBS. At week 3 when mice developed palpable tumors, mice received either a mouse monoclonal anti-YKL-40 antibody (mAY, 5 mg/kg body weight) or mouse IgG (5 mg/kg) by subcutaneous injection twice a week for 2 weeks. Tumor growth from these injected cells was monitored weekly for 5 weeks before the animals were humanely sacrificed. Tumors were measured and tumor volume was calculated as follows: volume = length × width^2 × 0.52.

Immunohistochemistry—Paraffin-embedded or frozen tumor tissues were cut to 6-μm thickness and processed for immunohis-

tochemical analysis. In brief, samples were incubated with 3% H_2O_2 for 30 min to block endogenous peroxidase activity, followed by incubation with blocking buffer containing 10% goat serum for 1 h. The samples then were incubated at room temperature for 2 h with monoclonal rat anti-CD31 (1:50, BD Pharmingen, San Diego, CA) and mouse anti-CD34 (1:200) antibodies (Dako Inc., Carpentaria, CA), or rabbit polyclonal anti-VEGF (1:100, Santa Cruz) and anti-YKL-40 (1:400). Goat anti-rat, mouse, or rabbit secondary antibodies (1:100, Dako Inc) conjugated to HRP were added for 1 h. Finally, dimethylaminoazobenzene substrate (Dako Inc.) was introduced for several minutes and after washing, methyl green was used for counterstaining.

Human Glioblastoma Samples and IHC Data Analysis—The study of brain tumor samples was approved by Baystate Medical Center Institutional Review Board. YKL-40 and VEGF staining was evaluated as combined scores of percent and intensity of positive staining cells as following: 1) % no staining is 0 points; <10% of cells stained is 1 point; 11–50% of cells stained is 2 points; and >50% of cells stained is 3 points; 2) intensity: no staining is 0 points, weak staining is 1 point, moderate staining is 2 points and strong staining is 3 points. Thus, the valid range of scores was 0 to 6. CD34 density was quantified by an NIH Image analysis program.

RESULTS

YKL-40 Regulates VEGF and Both Synergistically Promote Angiogenesis—Two brain tumor cell lines, U87 and SNB-75, were utilized to investigate a functional role of secreted angiogenic factors YKL-40 and VEGF in glioblastoma development. YKL-40 was highly detectable in both cell lines at the protein and mRNA levels, whereas other cell lines did not express YKL-40 or a low level of YKL-40. VEGF was expressed in those two brain tumor lines as well as osteoblastoma cell MG-63 and colon cancer cell HCT-116 (Fig. 1*A*). To validate that these angiogenic factors are associated with tumor angiogenesis, each brain tumor cell line was injected subcutaneously into SCID/Beige mice and tumors were monitored weekly for 8 weeks. Immunohistochemical (IHC) analysis showed strong expression of YKL-40 and VEGF, and extensive positive staining of CD31, a marker of vascular endothelial cells, in xenografted tumors (Fig. 1*B*), suggesting that both YKL-40 and VEGF may contribute to tumor development through a synergistic mechanism on the development of angiogenesis.

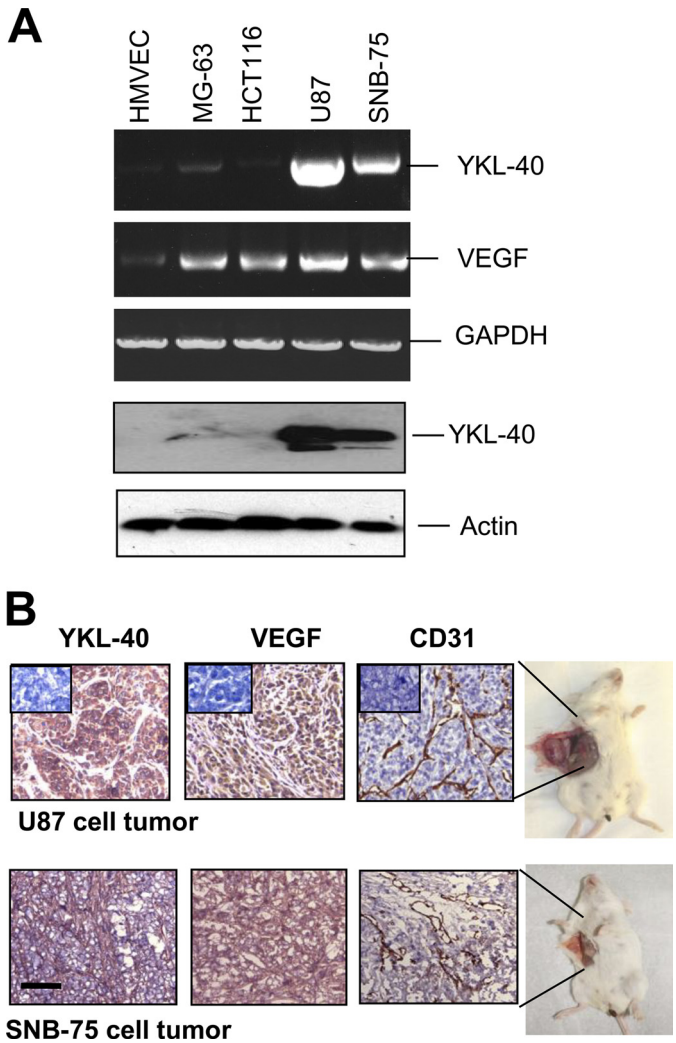

FIGURE 1. **YKL-40 and VEGF are highly expressed in two glioblastoma cell lines and in both cell line-induced vascular tumors.** *A*, *YKL-40* mRNA and protein levels, and *VEGF* mRNA levels were analyzed using RT-PCR and Western blot in HMVEC, MG-63, HCT-116, U87, and SNB-75 cells. Actin and GAPDH were used as loading controls for the Western blot and RT-PCR, respectively. *B*, U87 and SNB-75 cells were injected subcutaneously into SCID/Beige mice. CD31 staining of mouse endothelial cells in both a U87 tumor and SNB-75 tumor demonstrated extensive vasculature throughout the tumors. YKL-40 and VEGF were also highly expressed in these tumor samples. *Insets* indicate negative controls. *Bar,* 200 μm.

To dissect the relationship between YKL-40 and VEGF in tumor angiogenesis, we employed a YKL-40 gene knockdown approach in U87 cells by a stable retroviral siRNA infection. A noticeable gene blockade was obtained in cells expressing YKL-40 siRNA1 (S1) (Fig. 2*A*). Conversely, engineering *YKL-40* siRNA2 (S2) into the cells did not result in a decrease of YKL-40 as compared with the control cells containing an empty vector (Fig. 2*A*). S1 cells displayed a corresponding reduction of VEGF, whereas S2 and control cell lines did not show altered VEGF (Fig. 2*A*), suggestive of a regulatory role of YKL-40 in VEGF expression. To test the possibility that VEGF may also in turn regulate YKL-40 expression constituting a positive feedback loop for vigorous angiogenesis, parental U87 cells were treated with a neutralizing anti-VEGF antibody. Interestingly, neutralization of VEGF activity with a short time (24 h) failed to decrease expression of YKL-40 or VEGF itself relative to IgG-treated cells (Fig. 2*B*); however, blockade of VEGF for 1 week noticeably induced YKL-40 expression (Fig. 2*C*). The results indicate that VEGF does not have the ability to regulate YKL-40 directly, but blocking VEGF for a long term up-regulates YKL-40. To assess angiogenic activities of YKL-40 in vascular endothelial cells, HMVECs were engaged to measure tube formation on Matrigel, the assay that recapitulates vascular angiogenic signature *in vivo*. U87 conditioned medium treated with an anti-VEGF antibody for 1 week moderately suppressed tube formation by ~35% of IgG-treated tubes (Fig. 2*C*, compared with a strong inhibition below), suggestive of a compensatory role played by YKL-40 in angiogenesis after the inhibition of VEGF. We next sought to determine the effects of both YKL-40 and VEGF on angiogenesis. S1 medium drastically inhibited

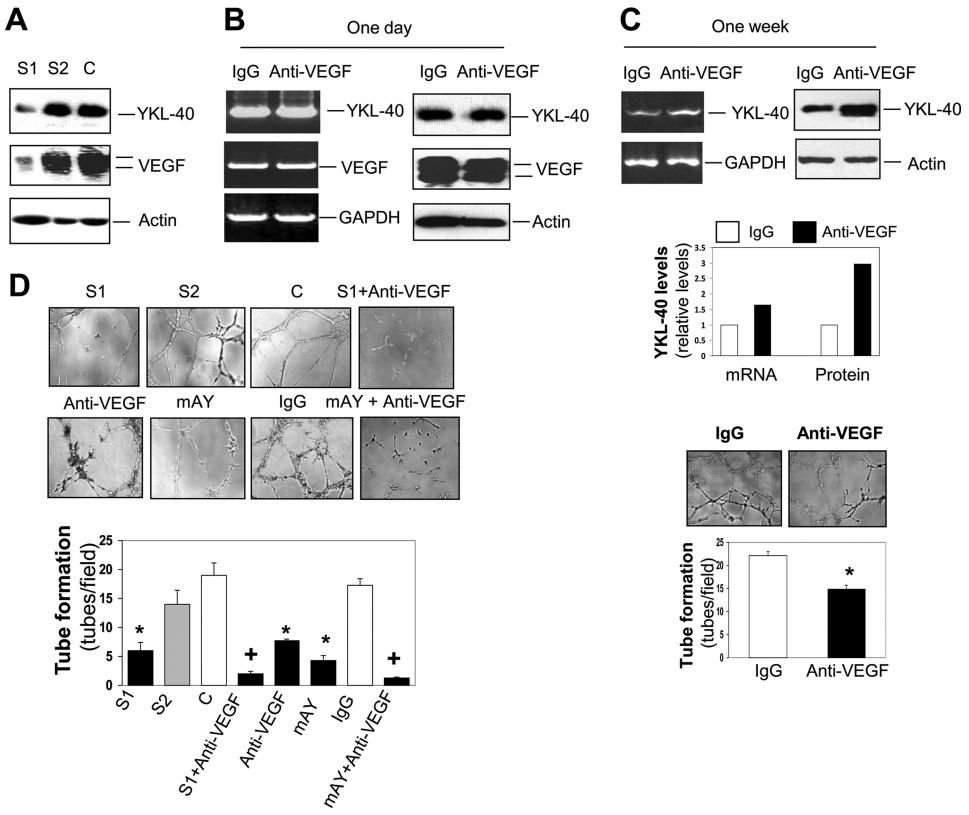

FIGURE 2. **YKL-40 regulates VEGF expression and both enhance angiogenesis *in vitro*.** *A*, YKL-40 regulates VEGF expression. The *YKL-40* gene was knocked down in U87 cells using two different siRNA constructs and YKL-40 and VEGF levels were detected using Western blotting. Actin was used as loading controls. *C*, *S1*, and *S2* represent vector control, *YKL-40* siRNA1, and *YKL-40* siRNA2, respectively. *B*, VEGF does not regulate YKL-40 directly. U87 cells were treated with an anti-VEGF neutralizing antibody for 24 h, and *VEGF* and *YKL-40* levels were tested using RT-PCR and immunoblotting. *C*, chronic blockade VEGF induces YKL-40. One week following treatment with an anti-VEGF antibody, conditioned medium was tested for YKL-40 expression and also for tube formation of HMVECs. Cell lysates were tested for mRNA levels of *YKL-40* using RT-PCR. *, $p < 0.05$ compared with IgG control, $n = 3$. *D*, YKL-40 and VEGF synergistically increase tube formation. HMVECs were placed on Matrigel in the presence of conditioned medium collected from U87 cell lines (*top row*) and allowed to grow for 16 h. Additionally, HMVECs were also grown on Matrigel with medium collected from control U87 cells pre-treated with anti-VEGF antibody, mAY, IgG (10 μg/ml), or a combination (*bottom row*). Tubes were counted for each condition. *, $p < 0.05$ compared with control or IgG group, and +, $p < 0.05$ compared with single treatment, $n = 3$.

tubules by 58–68% relative to the medium from S2 or control cells (Fig. 2*D*). To firmly establish the role of YKL-40 and VEGF in angiogenesis *in vitro*, neutralizing monoclonal antibodies against VEGF and YKL-40 (mAY) were added to the conditioned medium of the U87 control cells for 16 h. In line with *YKL-40* gene knockdown, anti-VEGF antibody suppressed tubules by 57% and mAY reduced tubules by 65% compared with IgG control (Fig. 2*D*). Combined treatments with the anti-VEGF antibody and YKL-40 siRNA or mAY strikingly suppressed tube formation by 88 and 93% relative to controls, respectively. Collectively, these data suggest that YKL-40 may have a role in the regulation of VEGF expression, both of which collaborate to enhance angiogenesis, and that blockade of VEGF induces YKL-40 expression.

YKL-40 Induces VEGF Expression and Angiogenesis through Signaling Activation of Integrin αvβ5, Syn-1, FAK, and ERK—In an attempt to define the molecular mechanisms by which YKL-40 regulates VEGF, we focused on signaling activation in U87 cells. Although membrane receptors specific for YKL-40 binding are still unknown, we have demonstrated that YKL-40 triggers coupling of membrane receptor Syn-1 and integrin $\alpha v\beta 3$ through binding to heparan sulfate of the ectodomains of Syn-1 in HMVECs (2). U87 cells expressed both Syn-1 and integrin $\alpha v\beta 3$ and $\alpha v\beta 5$ (supplemental Fig. S1). However, *YKL-40* gene knockdown did not have an impact on the expression of either receptor. To determine whether YKL-40 induces the coordination of these receptors, we utilized a co-immunoprecipitation approach followed by immunoblotting. We surprisingly found that both control and S2 cells demonstrated a strong association of Syn-1 with integrin $\alpha v\beta 5$, whereas S1 cells were defective in their interaction (Fig. 3*A*). In contrast, neither control nor *YKL-40* siRNA cells exhibited the interaction between Syn-1 and integrin $\alpha v\beta 3$ (Fig. 3*A*). These data provide strong evidence revealing the specificity of this signaling pathway that is dependent on individual cell types. To further identify intracellular signaling pathways, we then measured FAK, ERK-1, and ERK-2. An active level of $pFAK^{397}$ was significantly reduced in S1 cells relative to control cells (Fig. 3*B*). Accordingly, pERK-1 and pERK-2 were decreased in S1 cells.

To validate this signaling pathway regulated by YKL-40, we neutralized YKL-40 activity using mAY in the control cells. mAY disrupted the coupling between integrin $\alpha v\beta 5$ and Syn-1 from as early as 10 to 60 min and this inhibition was slightly diminished at 6 h (Fig. 3*C*). Consistent with this inhibition, $pFAK^{397}$, pERK-1, and pERK-2 were decreased by mAY, in which $pFAK^{397}$ displayed a trend to recovery from 30 min to

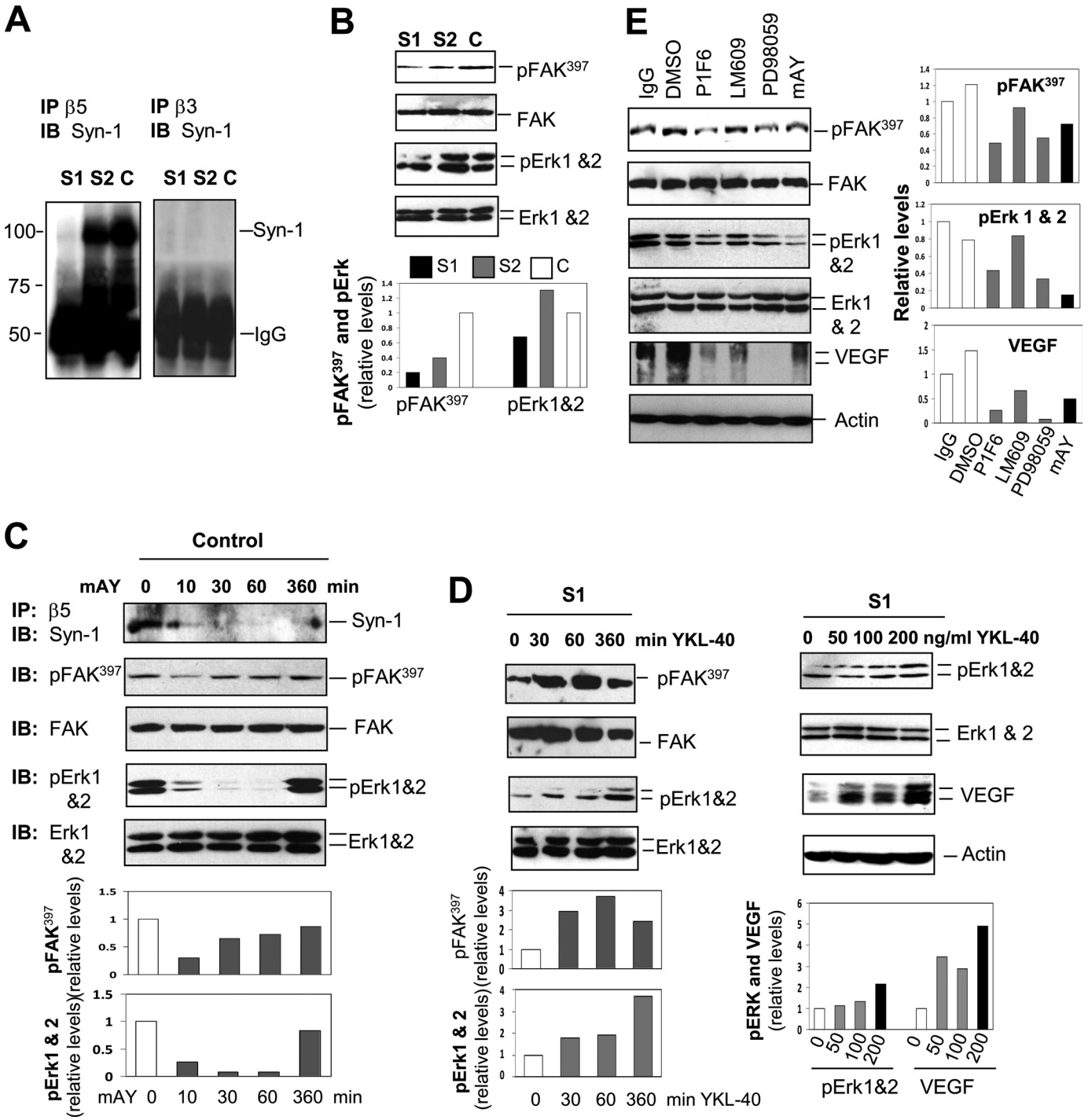

FIGURE 3. **YKL-40 increases VEGF expression by signaling through integrin αvβ5, Syn-1, FAK, and ERK.** *A*, YKL-40 signals through Syn-1 and integrin αvβ5 but not integrin αvβ3. Baseline immunoprecipitation (*IP*) of integrin β5 and β3 was performed on the U87 cell lysates, followed by Western blotting against Syn-1. The bands of IgG were used as loading controls. *B,* YKL-40 knockdown decreases expression of pFAK and pERK. pFAK, total FAK, pERK-1, pERK-2, total ERK-1, and ERK-2 protein levels were tested in the cells. pFAK, pERK-1, and -2 were quantified by normalizing with total FAK, ERK-1, and -2, respectively. Control pFAK and pERK were set up as 1 unit. *C*, neutralization of YKL-40 by mAY inhibits YKL-40 signaling. U87 control cells were treated with mAY (10 μg/ml) from 10 to 360 min and then some of cell lysates were immunoprecipitated with an anti-integrin β5 antibody followed by immunoblotting (*IB*) against Syn-1. The remaining lysates were subjected to immunoblotting using anti-pFAK, total FAK, pERK, and total ERK antibodies. pFAK and pERK were quantified as described in *B*. *D,* addition of recombinant YKL-40 protein to S1 cells increases pFAK, pERK-1, pERK-2, and VEGF protein levels. S1 cells were treated with YKL-40 (200 ng/ml) from 30 to 360 min. Cell lysates were analyzed for expression of pFAK, total FAK, pERK, and total ERK followed by quantification of pFAK and pERK as described in *B*. In addition, S1 cells were treated with 0, 50, 100, or 200 ng/ml of recombinant YKL-40 for 24 h. pERK, total ERK, and VEGF protein levels were tested by Western blotting. pERK-1, pERK-2, and VEGF were normalized with total ERK-1, ERK-2, and actin, respectively. Each expression level without YKL-40 treatment was set up as 1 unit. *E*, inhibition of integrin αvβ5, ERK, or YKL-40 results in reduced pFAK, pERK-1, pERK-2, and VEGF protein levels. Control U87 cells were treated with PD98059 (MEK inhibitor, 10 μM) or a monoclonal neutralizing antibody against integrin αvβ5 (P1F6), integrin αvβ3 (LM609), or YKL-40 (mAY) (10 μg/ml) for 24 h. Media samples and cell lysates were collected and Western blotting was performed to determine pFAK, pERK-1, pERK-2, total FAK, ERK-1, ERK-2, and VEGF protein levels. Actin was tested as a loading control. pFAK, pERK-1, pERK-2, and VEGF were normalized with total FAK, ERK-1, ERK-2, and actin, respectively. Control IgG values in each expression were set up as 1 unit.

6 h, whereas pERK-1 and pERK-2 recovered at 6 h (Fig. 3*C*). To determine whether YKL-40 is able to rescue the signaling impaired in S1 cells, we exposed these cells to recombinant YKL-40 and found that $pFAK^{397}$ was notably increased from 30 to 60 min; then slightly reduced (Fig. 3*D*). Like mAY blockade, a delayed response of pERK-1 and pERK-2 to YKL-40 stimulation was observed at 6 h (Fig. 3*D*), suggesting a downstream signaling pathway from FAK to ERK. To ensure that prolonged treatment of S1 cells with YKL-40 can restore VEGF production, these cells were exposed to recombinant YKL-40 for 24 h. YKL-40 induced expression of pERK-1, pERK-2, and VEGF in a dose-dependent manner (Fig. 3*D*).

Next, to determine whether the "outside-in" signaling pathway initiated by YKL-40 mediates VEGF expression, we engaged a series of different inhibitors specific for individual signaling mediators, which include a small molecule PD98059 targeting MEK, and neutralizing antibodies against YKL-40 (mAY), integrin $\alpha v\beta 3$ (LM609), and $\alpha v\beta 5$ (P1F6). Neutralization of integrin $\alpha v\beta 5$, MEK, or YKL-40 resulted in reduction of $pFAK^{397}$, pERK-1, pERK-2, and VEGF expression compared with IgG or dimethyl sulfoxide-treated controls (Fig. 3*E*). Interestingly, LM609 also moderately inhibited VEGF expression, implicating that other factors may also utilize integrin $\alpha v\beta 3$ in the induction of VEGF. Taken together, these results have established an action model for YKL-40 in the regulation of VEGF, in which YKL-40 promotes the coordination of Syn-1 and integrin $\alpha v\beta 5$, and induces intracellular signaling of FAK, ERK-1, and ERK-2, leading to VEGF expression.

YKL-40 Protects γ-Irradiation-induced Cell Death in an AKT-dependent Manner—It was established that serum levels of YKL-40 were elevated in glioblastoma patients treated with radiation therapy (34). Furthermore, these elevated concentrations positively correlated with cancer recurrence and poor survival, suggesting that serum levels of YKL-40 serve as a prognostic biomarker (43). To test the hypothesis that γ-irradiation-induced YKL-40 protects tumor cell death, we monitored the levels of YKL-40 in U87 cells exposed to γ-irradiation. Treatment of control cells with γ-irradiation resulted in an increase of YKL-40 with the strongest induction at 10 Gy γ-irradiation (Fig. 4*A*) but not 20 Gy γ-irradiation (data not shown). In contrast, γ-irradiation was unable to markedly induce YKL-40 expression in S1 cells. Although the control cells constantly expressed high levels of VEGF, regardless of the treatment with different doses of γ-irradiation, S1 cells did show a notable reduction in VEGF and exposure of the S1 cells with γ-irradiation failed to induce VEGF dramatically, underscoring an important role of YKL-40 in the regulation of VEGF during radiotherapy. Next, to test if YKL-40 acts as a survival factor in radiation treatment, both control and S1 cells were challenged with 10 Gy γ-irradiation for 48 h. Control cells experienced minimal cell death at 0 and 10 Gy γ-irradiation (Fig. 4, *B* and *C*). However, the S1 cells suffered 25 and 35% cell death at 0 and 10 Gy γ-irradiation, respectively (Fig. 4, *B* and *C*), both of which increased cell death ~2.5–3-fold greater than corresponding control cells; demonstrating a survival function played by YKL-40. Given that YKL-40 controls VEGF expression, we tested if VEGF mediates YKL-40-induced cell survival. A neutralizing anti-VEGF antibody was engaged, but it did not influence cell death in the control cells treated with γ-irradiation (Fig. 4*D* and supplemental Fig. S2*A*). These data indicate that YKL-40 protects γ-irradiation-induced cell death in a VEGF-independent manner.

To explore a molecular mechanism underlying cell survival, we focused on expression of PI3K and AKT, the common signaling pathways mediating cell survival. Strikingly, 10 Gy γ-irradiation up-regulated pAKT by 50% in the control U87 cells, whereas the treatment dramatically reduced expression of pAKT in the S1 cells compared with the levels after treatment with or without γ-irradiation in the control cells (Fig. 4*E*). Interestingly, whereas PI3K protein levels were not altered in cells exposed to γ-irradiation, PI3K kinase activity was decreased by 30% compared with controls when treatment of both γ-irradiation and *YKL-40* siRNA (Fig. 4*E*), suggesting that YKL-40 protects cell death induced by γ-irradiation at least partially through regulation of the PI3K-AKT pathway. Consistent with evidence that VEGF did not mediate YKL-40-induced cell survival, neither AKT nor PI3K were altered in the inhibition of VEGF (supplemental Fig. S2*B*). To further assess if γ-irradiation-induced YKL-40 consequently influences endothelial cell angiogenesis, which recapitulates YKL-40-induced angiogenesis via a paracrine fashion *in vivo*, we examined effects of conditioned medium from the irradiated U87 cells on tubules formed by HMVECs on Matrigel. Consistent with earlier findings (Fig. 2*D*), conditioned medium of S1 cells decreased 50% of the control tubules (Fig. 4*F*). Markedly, conditioned medium of U87 cells treated with γ-irradiation induced tubules by 60% relative to non-γ-irradiation-treated medium. But S1 cell medium treated with γ-irradiation suppressed these tubules to the non-treated basal levels. In summary, all data demonstrate that YKL-40 induced by γ-irradiation prompts tumor cell survival through a PI3K-AKT pathway, and concomitantly stimulates endothelial cell angiogenesis.

To further confirm the survival activity played by YKL-40 in radioresistance, we treated U87 parental cells with mAY with 10 Gy irradiation exposure for 96 h. In line with the S1 and control U87 data above, neutralization of YKL-40 activity led to 60% cell death compared with 40% cell death in the absence or presence of IgG after 10 Gy γ-irradiation (Fig. 5), strengthening the findings that YKL-40 protects γ-irradiation-induced cell death and that mAY may serve as a powerful therapeutic tool to treat radioresistant cancer patients.

YKL-40 Promotes Tumor Growth, Angiogenesis, and Metastasis in Vivo—Although the *in vitro* evidence established thus far has demonstrated that YKL-40 mainly controls angiogenesis, we then sought to ascertain the vital role played by YKL-40 with respect to tumor angiogenesis and progression *in vivo*. We performed two distinct mouse models for the study. In the first model, we attempted to mimic a clinical trial for the treatment of GBM by administering mAY into U87 xenografted mice from week 3 when these mice developed palpable tumors. Mice were given either 5 mg/kg of mAY or a monoclonal IgG as controls twice a week for 2 more weeks prior to sacrifice. mAY treatment significantly inhibited tumor formation as 50% of tumor volume was decreased compared with tumors developed from mice treated with IgG (Fig. 6*A*). To corroborate the *in vitro* data, we stained CD31 expression for angiogenesis in

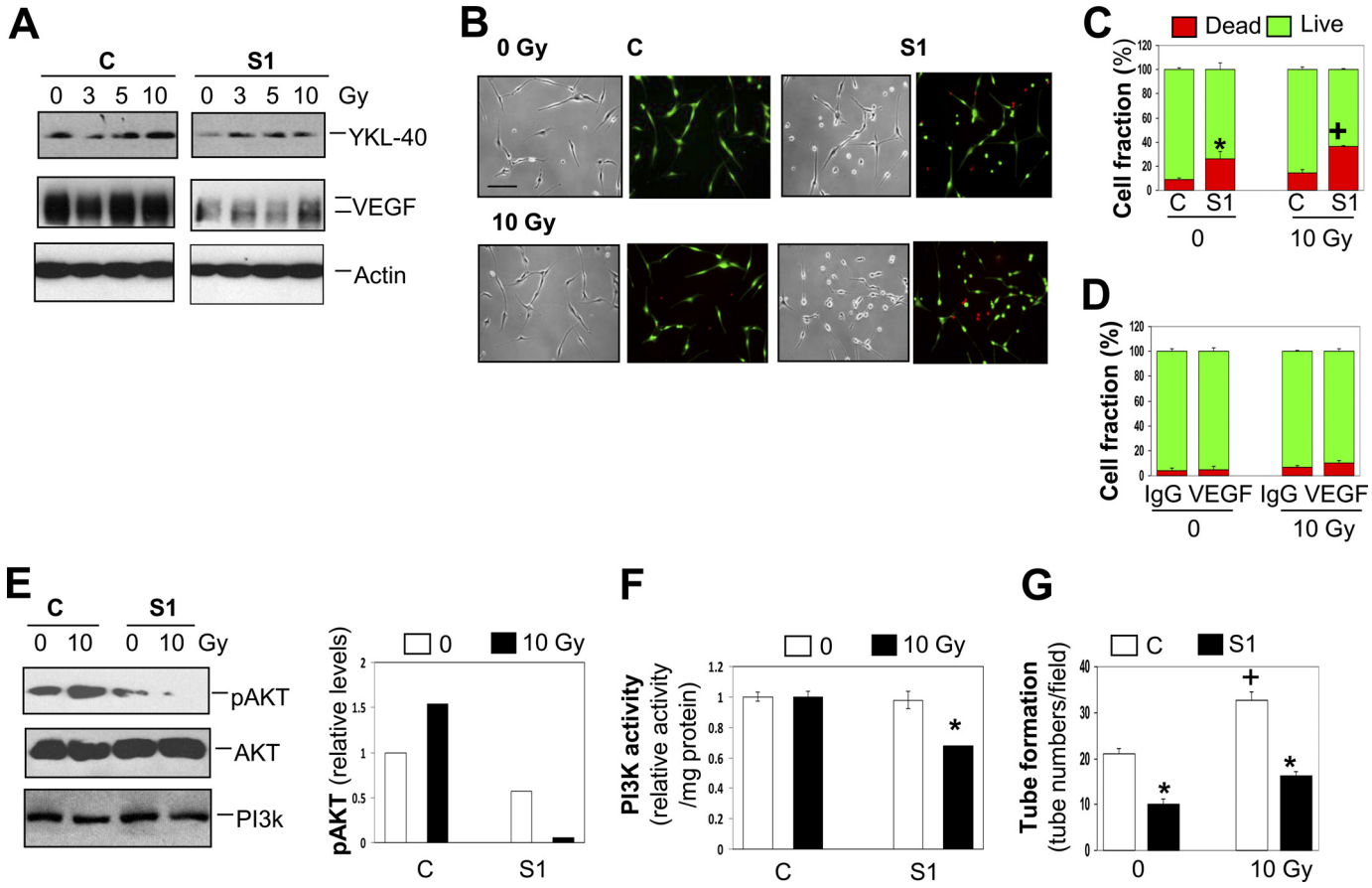

FIGURE 4. **YKL-40 protects U87 control cells from irradiation-induced death.** *A*, YKL-40, but not VEGF, is up-regulated with irradiation. U87 control and S1 cells were exposed to 0, 3, 5, or 10 Gy irradiation and samples were collected 48 h after irradiation. YKL-40 and VEGF protein levels were tested by Western blotting. Actin was used as a loading control. *B* and *C*, U87 S1 cells are more susceptible to irradiation. Both U87 control and S1 cells were plated and exposed to 0 or 10 Gy irradiation. Forty-eight h later, the live/dead assay was employed to determine cell viability. The results were then quantified. * and +, $p < 0.05$ compared with controls without irradiation and S1 without irradiation, respectively, $n = 3$. *D*, VEGF does not mediate YKL-40-induced cell survival. U87 control cells were plated and exposed to 0 or 10 Gy irradiation in the absence or presence of an anti-VEGF antibody. Forty-eight h later, the live/dead assay was employed to determine cell viability. The results were then quantified, $n = 3$. *E*, YKL-40 regulates pAKT levels and PI3K activity in cells exposed to γ-irradiation. Cell lysates were collected 48 h after 0 or 10 Gy irradiation. pAKT, total AKT, and PI3K were tested by Western blotting. The levels of pAKT were normalized with total AKT and the control level of pAKT without irradiation treatment was set up as 1 unit. *F*, treatment of both irradiation and YKL-40 knockdown leads to suppression of PI3K activity. U87 cells were exposed to irradiation for 48 h and then lysed for analysis of PI3K activity. The activity was normalized with a control level without irradiation as 1 unit. $p < 0.05$ compared with any group, $n = 3$. *G*, endothelial cell tube formation is increased by irradiation of U87 cells, but decreased by *YKL-40* siRNA. HMVECs were plated onto Matrigel in the presence of conditioned medium collected from U87 control and S1 cells exposed to 0 or 10 Gy irradiation. Tubes were allowed to form for 16 h. The number of tubes was counted for each condition. *, $p < 0.05$ compared with controls and +, $p < 0.05$ compared with 0 Gy control, $n = 3$.

tumor samples, and IHC analysis revealed that mAY markedly reduced CD31 levels compared with the IgG counterpart, as the staining intensity was 25% of the control group (Fig. 6, *B* and *C*). Furthermore, in the analysis of ectopic tumor development, the mAY reduced liver metastasis by 40%, whereas all IgG-treated control animals grew massive tumor cells in the liver (Fig. 6, *B* and *C*). Neither IgG- nor mAY-treated mice were found to contain disseminating tumor cells in the lung (Fig. 6*B*). These data strongly support the notion that mAY can be used as a therapeutic agent targeting angiogenesis and metastasis in advanced tumors.

In the second xenografted model, we injected U87 control and S1 cells into mice to determine how *YKL-40* gene knockdown would affect tumor development *in vivo*. As demonstrated in Fig. 6*D*, all animals receiving U87 control cells began to form tumors from week 4 and continued to develop exponentially large tumors until the mice were sacrificed by week 7. Conversely, only one of the six mice injected with U87 S1 cells exhibited a 2-week delayed tumor (Fig. 6*D*, *gray diamonds*). Surprisingly, the remainder of these animals failed to form tumors even after the observation period was extended to 11 weeks. Subsequently, IHC analysis of angiogenesis in all control tumors indicated strong staining of CD31 and VEGF (Fig. 6*E*); whereas one S1 tumor sample showed weak expression of CD31 and VEGF (supplemental Fig. S3). Furthermore, liver metastasis was identified in three of six control mice contrary to S1 mice in which one of six individual liver samples harbored tumor cells (Fig. 6*E*). Taken together, these mouse models suggest that YKL-40 is associated with tumorigenesis, angiogenesis, and metastasis.

Elevated Expression of YKL-40 Is Associated with Increased VEGF and Poorer Survival of Glioblastoma Patients—We finally aimed to explore the relationship of YKL-40 with VEGF production, tumor angiogenesis, and tumor malignancy in patients with glioblastomas. Tumor samples from 12 patients diagnosed with glioblastomas were utilized for expression of

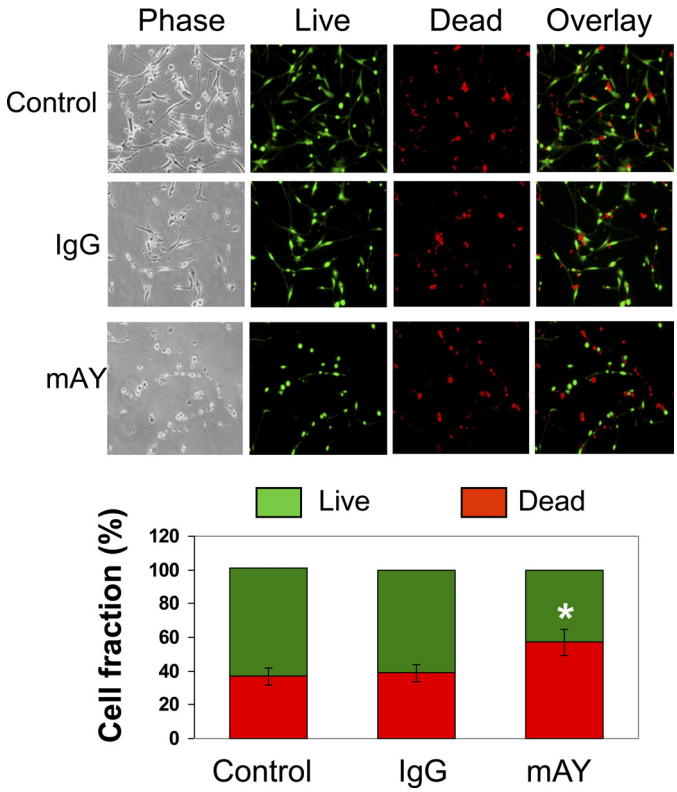

FIGURE 5. **A monoclonal neutralizing antibody against YKL-40 increases sensitivity of U87 cells to irradiation.** U87 cells were treated with IgG, mAY, or neither (*control*) and then exposed to 10 Gy irradiation. Ninety-six h later, the cells were subjected to the live/dead assay. Representative images were exhibited for each condition (*top*) and then the number of live and dead cells was quantified (*bottom*). *, $p < 0.05$ compared with control or IgG, $n = 3$.

YKL-40 and VEGF by immunoblotting. Given that variable levels of YKL-40 were observed in these specimens, we classified each patient into two categories: low YKL-40 expression (L) and high YKL-40 expression (H) (Fig. 7*A*). An analysis of patient survival showed a median survival of 14.6 *versus* 5.9 months in these two groups, demonstrating that elevated YKL-40 positively correlated with poor patient survival (Fig. 7*B*). YKL-40 levels also appeared to correlate with VEGF expression (Fig. 7*B*). To validate the association of these angiogenic factor levels with tumor angiogenesis, we stained these tumor samples for YKL-40, VEGF, and CD34 levels by IHC. In agreement with the immunoblotting data, the higher the YKL-40 expression, the higher the VEGF expression, and the more extensive the vessels appeared to be (Fig. 8*A*). YKL-40 levels in the immunoblotting analysis were in parallel with YKL-40 expression analyzed by IHC (Fig. 8*B*), confirming the specificity of a polyclonal anti-YKL-40 antibody in recognizing YKL-40 in tumors and also establishing these two sensitive assays for a diagnostic purpose. Statistical analyses of YKL-40, VEGF, and CD34 expression displayed a trend toward positive correlations based on these available samples (Fig. 8*B*). Collectively, these human data supported our hypothesis that YKL-40 plays a principal role in the regulation of VEGF, the strong vasculature phenotype, and tumor malignancy.

DISCUSSION

YKL-40 was recently identified as a potent angiogenic factor capable of inducing endothelial cell angiogenesis in breast cancer, independent of VEGF (2). Our current study demonstrates for the first time the regulatory mechanisms of these two important angiogenic factors in the malignancy of glioblastoma characterized by strong vascular proliferation. We have identified that YKL-40 up-regulates VEGF, and YKL-40-induced tumor angiogenesis is at least partially dependent on VEGF by means of a multidisciplinary approach including pharmacological and genetic methods, xenograft models *in vivo*, and human tumor samples. In addition, YKL-40 induced by γ-irradiation is the key component responsible for tumor radioresistance, independent of VEGF. mAY can block YKL-40-induced angiogenesis and metastasis. These findings have provided substantial evidence to elucidate the phenomena reported previously that serum and tissue levels of YKL-40 in glioblastomas are markedly elevated and these increased levels positively correlate with radioresistance and shorter survival (33, 43). Therefore, the current study not only provides mechanistic insights into the angiogenic properties of glioblastoma; but also establishes YKL-40 as a tumor diagnostic and prognostic biomarker in tumor radioresistance as well as a novel target for anti-angiogenic therapy.

With respect to the regulation of VEGF and angiogenesis, YKL-40 was found to induce the collaboration of Syn-1 with integrin $\alpha v\beta 5$ and then elicit intracellular signaling cascades through $pFAK^{391}$ to MAP kinase. This action model is highly consistent with our previous findings that the coupling of Syn-1 with integrin $\alpha v\beta 3$, in addition to $pFAK^{861}$ to MAPK, mediates YKL-40-induced angiogenic responses in vascular endothelial cells (2). Interestingly, LM609, the anti-integrin $\alpha v\beta 3$ antibody, was also found to partially reduce VEGF expression in U87 cells, implying that other factors may also induce signals through integrin $\alpha v\beta 3$ to regulate VEGF. This hypothesis was supported previously by multiple lines of *in vitro* and *in vivo* evidence (44, 45). For example, integrin $\alpha v\beta 3$ signaling was demonstrated to constitutively up-regulate VEGF expression in MDA-MB-435 breast cancer cells implanted into SCID mice (45). Indeed, we found that treatment of U87 cells with mAY alone failed to fully block VEGF expression (Fig. 3*C*) or tube formation induced by both YKL-40 and VEGF (Fig. 2*D*). Nevertheless, we demonstrate that YKL-40 plays a predominant role in the regulation of VEGF and angiogenesis. In addition, our data highlight the notion that the receptor cross-talk model is essential for the transduction of YKL-40 outside-in signaling into the cells, in which divergent signaling mediators participate in distinct functions (Fig. 9).

We found that γ-irradiation induced YKL-40 expression that not only protected tumor cell death, but also elicited endothelial cell angiogenesis in a paracrine fashion. This YKL-40-induced tumor cell survival was independent of VEGF, a factor that mediates endothelial cell survival (46). However, this survival activity was through PI3K-AKT activation, a common pathway that mediates survival of multiple types of cells (47, 48). Consistent with our results, MAPK and AKT were reported to mediate YKL-40-induced survival in tumor cells and mitogenic signaling in connective tissue cells (8, 49). In addition, IHC analysis of glioblastomas indicated that elevated expression of YKL-40 correlated with expression levels of pAKT and pMAPK in a poorer response for those patients to radiotherapy

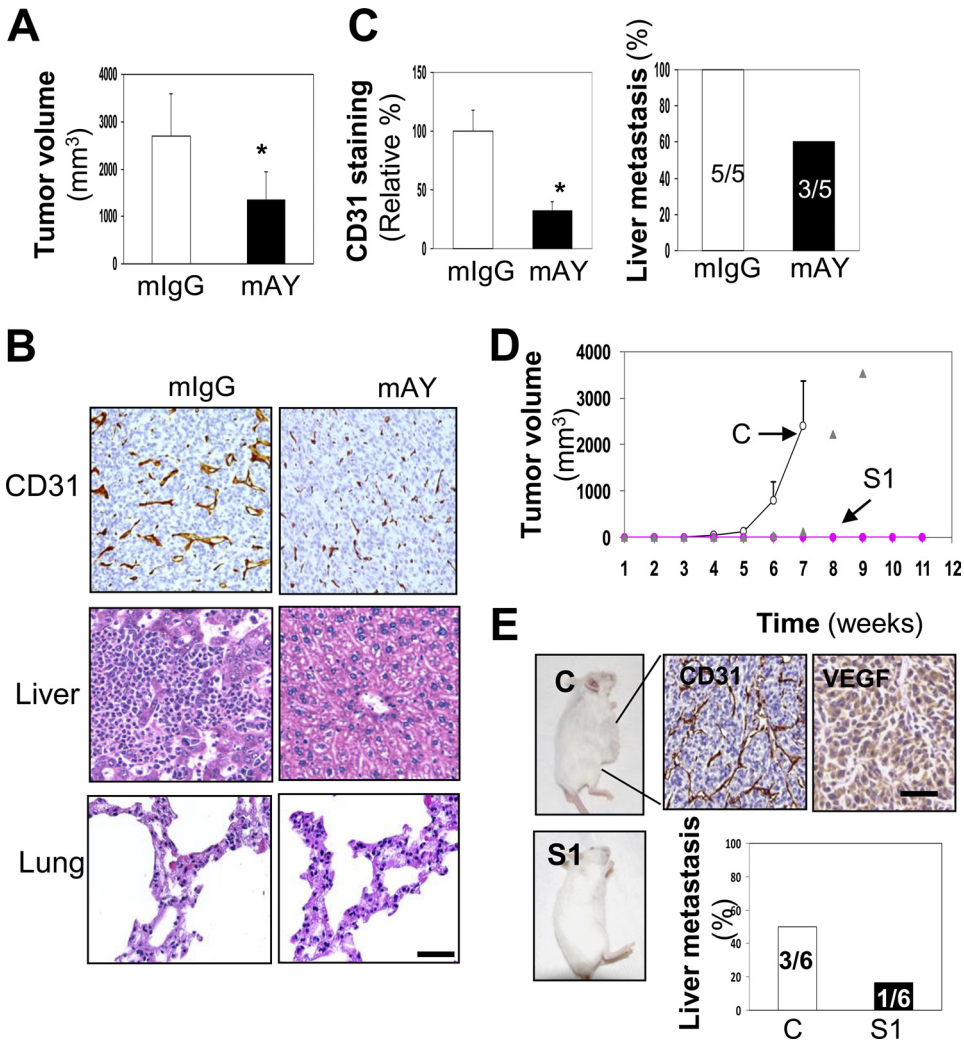

FIGURE 6. **YKL-40 is associated with increased tumor development and angiogenesis in two xenografted mouse models.** *A*, mAY reduces tumor volume. U87 parental cells were subcutaneously injected into SCID/Beige mice and once tumors developed by week 3, the animals were treated with 5 mg/kg of mAY or IgG by subcutaneous injection twice a week for 2 weeks. Mouse volume was shown at the end of the treatment. *B*, tumor angiogenesis and liver metastasis are reduced with mAY treatment. IHC analysis of CD31 was performed on mouse tumor samples from the IgG and mAY groups. H & E staining was performed on liver tissues from each group as well. *Bar*, 200 μm. *C*, quantification of *B*. *, $p < 0.05$ compared with controls, $n = 5$. *D*, *YKL-40* S1 knockdown inhibits tumor formation. U87 control and S1 cells were subcutaneously injected in SCID/Beige mice and observed for tumor development over 11 weeks. All control mice formed tumors within 7 weeks; whereas only 1 of 6 S1 mice formed a tumor between weeks 7 and 9, and the remaining mice did not form palpable tumors over 11 weeks. *Open circles* represent control mice, *triangles* represent the only one S1 mouse that formed a tumor, and *pink diamonds* indicate the other five S1 mice. *E*, U87 control tumors express high levels of CD31 and VEGF. IHC of CD31 and VEGF was performed on the tumor tissue of the U87 control mice. Liver metastasis was quantified as well for the U87 control and S1 cells (staining images of tumor cells were not shown). *Bar*, 100 μm.

(16, 50). Therefore, our new data in context with others offered substantial insight into radioresistance of glioblastomas that express increased levels of YKL-40 and demonstrate poor prognosis (Fig. 9).

mAY has been characterized in neutralizing the activities of YKL-40 (56). Here, mAY displays the capability of blocking tumor angiogenesis and growth *in vivo* but failed to resemble the inhibitory extent of *YKL-40* gene knockdown that completely abolished the tumor development. The discrepancy may be attributed to different settings on YKL-40 inhibition, in which mAY targets palpable tumors contrary to the siRNA approach that genetically decreases *YKL-40* levels in the tumor cells. We also interestingly found that subcutaneous injection with U87 cells gave rise to liver metastasis but not lung metastasis, which is different from metastases of other tumor cells that disseminated to the lung and other organs (51–53). The inconsistency may be due to the differences in administration methods of xenotransplants, invasiveness of tumor cells, and the tumor microenvironment that predisposes them to residing in specific sites. Nonetheless, our data demonstrate that blockade of YKL-40 expression or activity suppresses tumor growth, angiogenesis, and metastasis. Moreover, the results also implicate the therapeutic utility of mAY in future clinical treatment.

Both immunoblotting and IHC analyses on 12 cases of glioblastomas revealed that half of these samples express strong YKL-40, the high population of which is consistent with the data documented in literature (16, 34). In addition, these elevated expression levels of YKL-40 positively correlate with poorer survival. The results demonstrate that these two tests can serve as diagnostic and/or prognostic tools for predicting the outcomes of the disease. A more detailed epidemiological analysis of YKL-40, VEGF, and CD34 with a large population

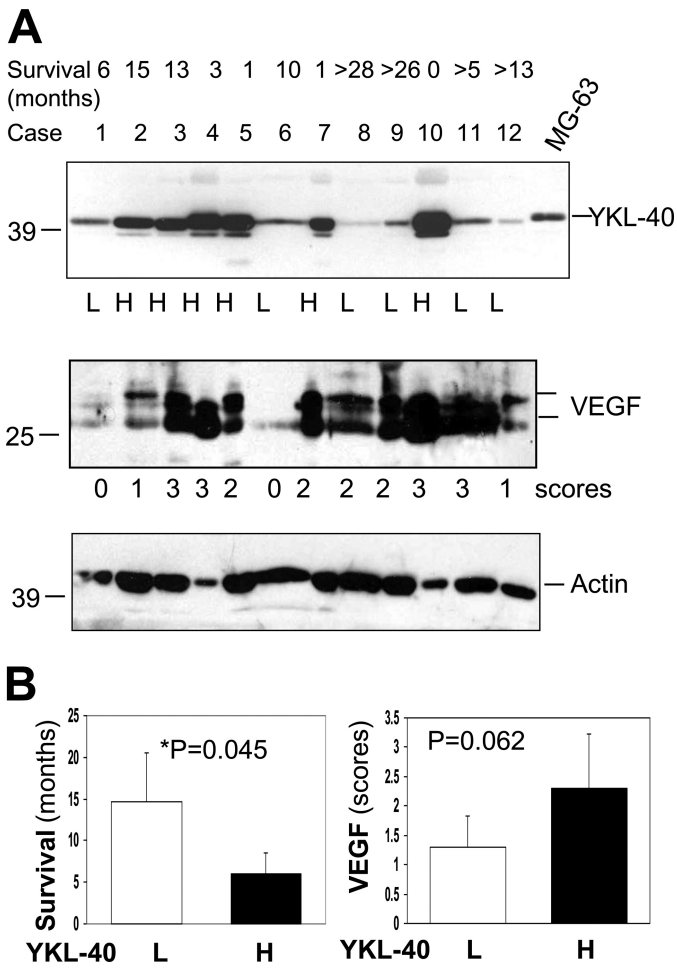

FIGURE 7. **YKL-40 and VEGF are overexpressed in glioblastoma patients with poorer survival.** *A*, YKL-40 and VEGF are expressed in glioblastoma patients. Protein samples were isolated from 12 glioblastoma tumor specimens and subjected to Western blotting. Actin was used as a loading control. MG63 osteosarcoma-conditioned medium was used as a positive control. Tumor samples were classified into two groups based on YKL-40 intensity: *L*, low expression and *H*, high expression. Additionally, VEGF was scored for band intensity as well: 0 = minimal level, 1 = low level, 2 = medium level, and 3 = high level of VEGF. *Top row* shows patient survival data. ">" indicates patients currently live longer than these months. *B*, elevated levels of YKL-40 are associated with decreased patient survival and possibly increased VEGF expression. *Left*, comparison of YKL-40 expression groups (low and high levels, *n* = 6/group) to average patient survival. *Right*, comparison of YKL-40 expression to VEGF levels.

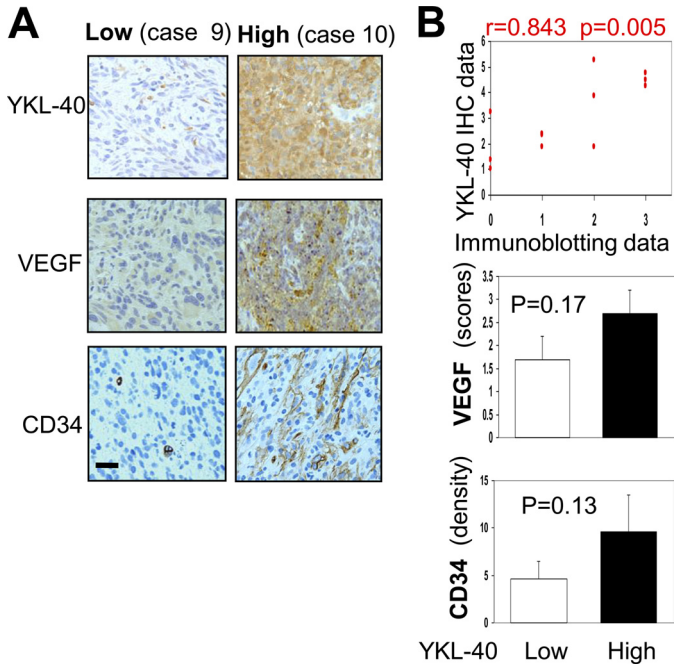

FIGURE 8. **YKL-40 levels appear to correlate with VEGF and CD34 levels.** *A*, immunohistochemical analysis of low and high YKL-40 patient cases. Representative tumor samples from low (*L*) or high (*H*) YKL-40 groups (see Fig. 7) were stained for YKL-40, VEGF, and CD34. *Bar*, 100 μm. *B*, *top*, YKL-40 staining of IHC was semiquantified with density (0–3 points) and intensity (0–3 points) scores as described under "Experimental Procedures," and YKL-40 bands of immunoblots (Fig. 7*A*) were analyzed based on intensity (0–3 points). The scores were then subjected to a linear regression analysis followed by significance analysis. *Bottom*, VEGF was semiquantified based on staining density and intensity (0–6 points) and CD34 was scored by overall staining density.

will be essential for establishing that YKL-40 has utility as a target for anti-angiogenic intervention in patients.

Insufficient anti-angiogenic therapy in glioblastoma patients has recently received considerable attention because the benefits of these agents such as the anti-VEGF antibody bevacizumab appear to be transitory (39, 54). These effects may be due to drug resistance, tumor re-growth, and rapid vasculature recovery once the therapy is terminated. In agreement with these clinical trials, xenografted tumor models provided convincing evidence demonstrating conflicting outcomes of anti-VEGF treatment, including extensive revascularization, increased invasiveness, and ectopic dissemination (37, 55). In line with this evidence, short-term therapy with sunitnib (VEGF receptor kinase inhibitor) and SU11248 (VEGF and PDGF receptor kinase inhibitor) accelerated local tumor invasion and multiple distant metastases after intravenous injection of tumor cells or removal of primary tumors (41). Immediate adaptation to the anti-angiogenic therapies is believed to be associated with the angiogenic switch by which tumors undergo robust revascularization and malignant transformation. Our data showing the up-regulation of YKL-40 following a long course of anti-VEGF treatment strongly suggests that YKL-40 may play an angiogenic role in the resistance of enduring anti-VEGF therapy. This assumption was also supported by a study of *VEGF* gene knockdown in U87 cells that expressed elevated YKL-40 compared with control cells (42). Therefore, an alternative neutralization of YKL-40 should be taken into account in the clinical setting for the possible elimination of this angiogenic rebound. A putative model has been illustrated demonstrating the enhanced tumor angiogenesis associated with YKL-40 (Fig. 9). YKL-40 acts as an independent angiogenic factor and simultaneously up-regulates VEGF expression; thereby giving rise to a synergistic impact on vascularization. In addition, tumors can rebound upon anti-VEGF treatment alone because of up-regulation of YKL-40 by decreased VEGF. Although molecular mechanisms underlying the induction of YKL-40 are still elusive, the levels of VEGF may be rate-limiting for YKL-40 regulation, possibly constituting a negative feedback loop. Thus, targeting both YKL-40 and VEGF could be an efficacious regimen in concert with radiotherapy to eventually eradicate this deadly disease.

In summary, our findings demonstrate the angiogenic signature for YKL-40 in a vascular phenotype of glioblastoma, the

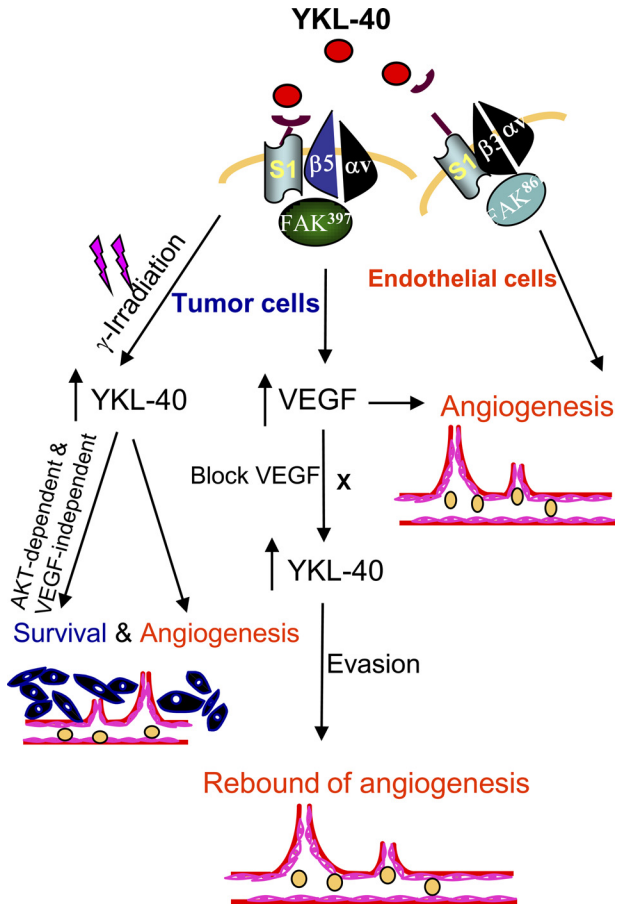

FIGURE 9. **A hypothetical scheme elucidating YKL-40-induced angiogenesis of glioblastoma, partially dependent on VEGF.** YKL-40 up-regulates VEGF, both of which synergistically induce endothelial cell angiogenesis, and YKL-40 also has the ability to directly promote angiogenesis as described previously (2). Constant inhibition of VEGF leads to up-regulation of YKL-40 that may stimulate rapid vascular recovery and tumor re-growth, which contributes to anti-VEGF resistance and evasive mechanisms for tumor malignancy. In addition, γ-irradiation induces YKL-40 expression that increases tumor cell survival and also promotes endothelial cell angiogenesis, leading to resistance to radiation therapy.

hallmark of tumor invasiveness. YKL-40 cannot only induce angiogenesis as an independent angiogenic factor, but also has the ability to stimulate VEGF expression, resulting in synergistic effects on angiogenesis. In addition, YKL-40 acts an important component to mediate the angiogenic rebound induced by anti-VEGF treatment as well as tumor radioresistance. Therefore, combined therapies including anti-YKL-40 and other traditional anti-angiogenic agents together with chemo/radiation therapy warrant further clinical investigation.

REFERENCES

1. Folkman, J., and Klagsbrun, M. (1987) *Science* **235,** 442–447
2. Shao, R., Hamel, K., Petersen, L., Cao, Q. J., Arenas, R. B., Bigelow, C., Bentley, B., and Yan, W. (2009) *Oncogene* **28,** 4456–4468
3. Yan, W., Bentley, B., and Shao, R. (2008) *Mol. Biol. Cell* **19,** 2278–2288
4. Dreyfuss, J. M., Johnson, M. D., and Park, P. J. (2009) *Mol. Cancer* **8,** 71
5. Johansen, J. S., Williamson, M. K., Rice, J. S., and Price, P. A. (1992) *J. Bone Miner. Res.* **7,** 501–512
6. Renkema, G. H., Boot, R. G., Au, F. L., Donker-Koopman, W. E., Strijland, A., Muijsers, A. O., Hrebicek, M., and Aerts, J. M. (1998) *Eur. J. Biochem.* **251,** 504–509
7. Fusetti, F., Pijning, T., Kalk, K. H., Bos, E., and Dijkstra, B. W. (2003) *J. Biol. Chem.* **278,** 37753–37760
8. Recklies, A. D., White, C., and Ling, H. (2002) *Biochem. J.* **365,** 119–126
9. De Ceuninck, F., Gaufillier, S., Bonnaud, A., Sabatini, M., Lesur, C., and Pastoureau, P. (2001) *Biochem. Biophys. Res. Commun.* **285,** 926–931
10. Malinda, K. M., Ponce, L., Kleinman, H. K., Shackelton, L. M., and Millis, A. J. (1999) *Exp. Cell. Res.* **250,** 168–173
11. Sharif, M., Granell, R., Johansen, J., Clarke, S., Elson, C., and Kirwan, J. R. (2006) *Rheumatology* **45,** 522–526
12. Johansen, J. S., Christoffersen, P., Møller, S., Price, P. A., Henriksen, J. H., Garbarsch, C., and Bendtsen, F. (2000) *J. Hepatol.* **32,** 911–920
13. Volck, B., Johansen, J. S., Stoltenberg, M., Garbarsch, C., Price, P. A., Ostergaard, M., Ostergaard, K., Løvgreen-Nielsen, P., Sonne-Holm, S., and Lorenzen, I. (2001) *Osteoarthritis Cartilage* **9,** 203–214
14. Kirkpatrick, R. B., Emery, J. G., Connor, J. R., Dodds, R., Lysko, P. G., and Rosenberg, M. (1997) *Exp. Cell Res.* **237,** 46–54
15. Létuvé, S., Kozhich, A., Arouche, N., Grandsaigne, M., Reed, J., Dombret, M. C., Kiener, P. A., Aubier, M., Coyle, A. J., and Pretolani, M. (2008) *J. Immunol.* **181,** 5167–5173
16. Pelloski, C. E., Mahajan, A., Maor, M., Chang, E. L., Woo, S., Gilbert, M., Colman, H., Yang, H., Ledoux, A., Blair, H., Passe, S., Jenkins, R. B., and Aldape, K. D. (2005) *Clin. Cancer Res.* **11,** 3326–3334
17. Cintin, C., Johansen, J. S., Christensen, I. J., Price, P. A., Sørensen, S., and Nielsen, H. J. (1999) *Br. J. Cancer* **79,** 1494–1499
18. Cintin, C., Johansen, J. S., Christensen, I. J., Price, P. A., Sørensen, S., and Nielsen, H. J. (2002) *Cancer* **95,** 267–274
19. Hogdall, E. V., Johansen, J. S., Kjaer, S. K., Price, P. A., Christensen, L., Blaakaer, J., Bock, J. E., Glud, E., and Hogdall, C. K. (2003) *Oncol. Reports* **10,** 1535–1538
20. Johansen, J. S., Christensen, I. J., Riisbro, R., Greenall, M., Han, C., Price, P. A., Smith, K., Brünner, N., and Harris, A. L. (2003) *Breast Cancer Res. Treat.* **80,** 15–21
21. Jensen, B. V., Johansen, J. S., and Price, P. A. (2003) *Clin. Cancer Res.* **9,** 4423–4434
22. Bergmann, O. J., Johansen, J. S., Klausen, T. W., Mylin, A. K., Kristensen, J. S., Kjeldsen, E., and Johnsen, H. E. (2005) *Clin. Cancer Res.* **11,** 8644–8652
23. Yancopoulos, G. D., Davis, S., Gale, N. W., Rudge, J. S., Wiegand, S. J., and Holash, J. (2000) *Nature* **407,** 242–248
24. Millauer, B., Longhi, M. P., Plate, K. H., Shawver, L. K., Risau, W., Ullrich, A., and Strawn, L. M. (1996) *Cancer Res.* **56,** 1615–1620
25. Neufeld, G., Cohen, T., Gengrinovitch, S., and Poltorak, Z. (1999) *FASEB J.* **13,** 9–22
26. Prewett, M., Huber, J., Li, Y., Santiago, A., O'Connor, W., King, K., Overholser, J., Hooper, A., Pytowski, B., Witte, L., Bohlen, P., and Hicklin, D. J. (1999) *Cancer Res.* **59,** 5209–5218
27. Guo, D., Jia, Q., Song, H. Y., Warren, R. S., and Donner, D. B. (1995) *J. Biol. Chem.* **270,** 6729–6733
28. Abedi, H., and Zachary, I. (1997) *J. Biol. Chem.* **272,** 15442–15451
29. Wheeler-Jones, C., Abu-Ghazaleh, R., Cospedal, R., Houliston, R. A., Martin, J., and Zachary, I. (1997) *FEBS Lett.* **420,** 28–32
30. Ilhan, A., Gartner, W., Neziri, D., Czech, T., Base, W., Hörl, W. H., and Wagner, L. (2009) *Anticancer Res.* **29,** 731–736
31. Zhao, J., Yan, F., Ju, H., Tang, J., and Qin, J. (2004) *Cancer Lett.* **204,** 87–95
32. Wen, P. Y., and Kesari, S. (2008) *New Engl. J. Med.* **359,** 492–507
33. Nigro, J. M., Misra, A., Zhang, L., Smirnov, I., Colman, H., Griffin, C., Ozburn, N., Chen, M., Pan, E., Koul, D., Yung, W. K., Feuerstein, B. G., and Aldape, K. D. (2005) *Cancer Res.* **65,** 1678–1686
34. Tanwar, M. K., Gilbert, M. R., and Holland, E. C. (2002) *Cancer Res.* **62,** 4364–4368
35. Lal, A., Lash, A. E., Altschul, S. F., Velculescu, V., Zhang, L., McLendon, R. E., Marra, M. A., Prange, C., Morin, P. J., Polyak, K., Papadopoulos, N., Vogelstein, B., Kinzler, K. W., Strausberg, R. L., and Riggins, G. J. (1999) *Cancer Res.* **59,** 5403–5407
36. Bao, S., Wu, Q., Sathornsumetee, S., Hao, Y., Li, Z., Hjelmeland, A. B., Shi, Q., McLendon, R. E., Bigner, D. D., and Rich, J. N. (2006) *Cancer Res.* **66,** 7843–7848
37. Pàez-Ribes, M., Allen, E., Hudock, J., Takeda, T., Okuyama, H., Viñals, F., Inoue, M., Bergers, G., Hanahan, D., and Casanovas, O. (2009) *Cancer*

Cell. **15,** 220–231
38. Ido, K., Nakagawa, T., Sakuma, T., Takeuchi, H., Sato, K., and Kubota, T. (2008) *Neuropathology* **28,** 604–611
39. Verhoeff, J. J., van Tellingen, O., Claes, A., Stalpers, L. J., van Linde, M. E., Richel, D. J., Leenders, W. P., and van Furth, W. R. (2009) *BMC Cancer* **9,** 444
40. Kreisl, T. N., Kim, L., Moore, K., Duic, P., Royce, C., Stroud, I., Garren, N., Mackey, M., Butman, J. A., Camphausen, K., Park, J., Albert, P. S., and Fine, H. A. (2009) *J. Clin. Oncol.* **27,** 740–745
41. Ebos, J. M., Lee, C. R., Cruz-Munoz, W., Bjarnason, G. A., Christensen, J. G., and Kerbel, R. S. (2009) *Cancer Cell* **15,** 232–239
42. Saidi, A., Javerzat, S., Bellahcène, A., De Vos, J., Bello, L., Castronovo, V., Deprez, M., Loiseau, H., Bikfalvi, A., and Hagedorn, M. (2008) *Int. J. Cancer* **122,** 2187–2198
43. Hormigo, A., Gu, B., Karimi, S., Riedel, E., Panageas, K. S., Edgar, M. A., Tanwar, M. K., Rao, J. S., Fleisher, M., DeAngelis, L. M., and Holland, E. C. (2006) *Clin. Cancer Res.* **12,** 5698–5704
44. Hood, J. D., Frausto, R., Kiosses, W. B., Schwartz, M. A., and Cheresh, D. A. (2003) *J. Cell Biol.* **162,** 933–943
45. Lorger, M., Krueger, J. S., O'Neal, M., Staflin, K., and Felding-Habermann, B. (2009) *Proc. Natl. Acad. Sci. U.S.A.* **106,** 10666–10671
46. Zhang, Z., Neiva, K. G., Lingen, M. W., Ellis, L. M., and Nör, J. E. (2010) *Cell Death Differ.* **17,** 499–512
47. Chetty, C., Lakka, S. S., Bhoopathi, P., and Rao, J. S. (2010) *Int. J. Cancer* **127,** 1081–1095
48. Inoue, T., and Meyer, T. (2008) *PLoS ONE* **3,** e3068
49. Li, H. F., Kim, J. S., and Waldman, T. (2009) *Radiat. Oncol.* **4,** 43
50. Pelloski, C. E., Lin, E., Zhang, L., Yung, W. K., Colman, H., Liu, J. L., Woo, S. Y., Heimberger, A. B., Suki, D., Prados, M., Chang, S., Barker, F. G., 3rd, Fuller, G. N., and Aldape, K. D. (2006) *Clin. Cancer Res.* **12,** 3935–3941
51. Minn, A. J., Gupta, G. P., Siegel, P. M., Bos, P. D., Shu, W., Giri, D. D., Viale, A., Olshen, A. B., Gerald, W. L., and Massagué, J. (2005) *Nature* **436,** 518–524
52. Richert, M. M., Phadke, P. A., Matters, G., DiGirolamo, D. J., Washington, S., Demers, L. M., Bond, J. S., Manni, A., and Welch, D. R. (2005) *Breast Cancer Res.* **7,** R819–827
53. Yan, W., and Shao, R. (2006) *J. Biol. Chem.* **281,** 19700–19708
54. Wick, W., Weller, M., van den Bent, M., and Stupp, R. (2010) *J. Clin. Oncol.* **28,** e188–189; author reply e190–192
55. Casanovas, O., Hicklin, D. J., Bergers, G., and Hanahan, D. (2005) *Cancer Cell.* **8,** 299–309
56. Fabish, M., Francescone, R., Bentley, B., Yan, W., and Shao, R. (2011) *Mol. Cancer Ther.*, in press